


Socioeconomic deprivation, brain morphology, and body fat among children and adolescents

Anting Yang^a, Hui Jing Lu^b, Lei Chang^{a,*} 

^a Department of Psychology, Faculty of Social Sciences Building E21B, University of Macau, Macao Special Administrative Region of China

^b Department of Applied Social Sciences, Faculty of Health and Social Sciences GH413, The Hong Kong Polytechnic University, Kowloon, Hong Kong, China

ARTICLE INFO

Keywords:

Life History Theory
Socioeconomic Status
Deprivation
Neural Development
Fat Deposition
Trade-Off

ABSTRACT

Given mounting literature linking environmental adversity with neurobiological alterations, other evidence has shown association between excess adiposity and attenuated brain development, leading to our current question of how the developing brain interacts with change in body composition in response to environmental challenges. Using data from the Adolescent Brain Cognitive Development (ABCD®) Study, we conducted mediation analyses and demonstrated that socioeconomic deprivation (SED) was associated with lower total brain and cortical volumes via the mediation of higher waist-to-height ratio (WHtR), and that WHtR likewise mediated the association of SED with global brain structures. The prefrontal structures showed region- and direction-specific pathways, with bilateral superior and middle frontal gyrus being most consistently related with WHtR in addition to the impact of SED. These findings reveal a functional trade-off between brain development and fat deposition in response to environmental deprivation, and may have implications for understanding neuro-cognitive and somatic development among children and adolescents in different socioeconomic contexts.

1. Introduction

The developing brain is sensitive to environmental inputs, especially during early periods of heightened neuroplasticity (Nelson & Gabard-Durnam, 2020; Reh et al., 2020). Deprivation, defined as lack of species-expected inputs from distal to proximal levels of material and social/cognitive exposure (e.g., local poverty, institutional rearing, neglect), may impact age-specific patterns of synaptic proliferation and pruning, resulting in neurobiological alterations and psychopathologies (Ellis et al., 2022; McLaughlin et al., 2014, 2019). As a form of material deprivation, low socioeconomic status (SES; e.g., neighborhood-level disadvantage, low family income, low parental education) has been exhibited to associate with lower cognitive and language stimulation (Rosen et al., 2020; von Stumm et al., 2020) and reduced cortical and subcortical structures (e.g., prefrontal cortex [PFC], anterior cingulate cortex [ACC], hippocampus; Lawson et al., 2013; McDermott et al., 2019; Miller et al., 2022; Noble et al., 2015; Taylor et al., 2020). Nonetheless, these atypical neural variations may also manifest as adaptive responses to environmental variation. Given the high energy requirements of the brain (Raichle & Gusnard, 2002), downregulating the metabolic costs of the brain by restricting neural development may

be adaptive under energy-deprived conditions, suggesting a developmental *trade-off* favoring maintenance at the expense of growth (Ellis et al., 2022). Following this *life history* (LH) perspective, we therefore raise questions of how neural development may relate to energy-allocation mechanisms and how their interactions may underlie adaptations to environmental deprivation.

One central tenet of the LH theory is that all living organisms face a biological constraint of a finite energy budget that cannot simultaneously fulfill increases in all life functions (e.g., growth, maintenance, reproduction; Del Giudice et al., 2015). This constraint drives organisms to maximize their fitness by prioritizing energy allocation to certain functions at the costs of others as per environmental condition, referred to as LH trade-offs (Del Giudice et al., 2015; Ellis et al., 2009). Specific to early stages of development is a trade-off between growth and maintenance (Bogin et al., 2007; Ellis et al., 2009; Geary, 2003). Growth is defined as increases in physical size, functional capacity, and energy-acquisition competence, whereas maintenance refers to energy expenditure on fundamental physiological processes that sustain immediate survival (e.g., metabolism, cellular repair, immune function). The trade-off of these two functions has been observed in smaller stature gains in indigenous children during periods of elevated immune activation (e.g.

* Corresponding author.

E-mail addresses: yc17305@um.edu.mo (A. Yang), huijing.lu@polyu.edu.hk (H.J. Lu), chang@um.edu.mo (L. Chang).

<https://doi.org/10.1016/j.bandc.2025.106315>

Received 17 January 2025; Received in revised form 29 April 2025; Accepted 9 May 2025

Available online 13 May 2025

0278-2626/© 2025 Elsevier Inc. All rights reserved, including those for text and data mining, AI training, and similar technologies.

C-reactive protein, immunoglobulin E; McDade et al., 2008; Shattuck-Heidorn et al., 2017; Urlacher et al., 2018; for a review see Pontzer & McGrosky, 2022).

This energy-allocation economics should also concern brain development because of the substantial energy consumption of brain tissue. With the human brain being multiple times larger than its body-expected size (Herculano-Houzel, 2012), it accounts for over 20 % of total basal metabolism (Niven, 2016; Raichle & Gusnard, 2002), roughly double the metabolic costs of the brain in other primates (Fonseca-Azevedo & Herculano-Houzel, 2012); this metabolic demand can even be two to three times higher during childhood (Kuzawa et al., 2014). An enlarged, energetically expensive brain may inherently compete with other somatic functions and tissues for energy (Isler & van Schaik, 2009; Peters et al., 2004). Kuzawa and colleagues (2014) reveal that brain metabolic demand (i.e., ratios of brain glucose uptake to the body's resting metabolic rate and daily energy expenditure) escalated since birth as the rate of weight growth declined; this inverse relationship became strongest when brain metabolic demand peaked (~ age 5 years), followed by a rebound of weight growth with decreasing brain metabolism. A later work has demonstrated similar inverse trajectories that total cerebral blood flow increased with lower body mass index and peaked roughly the time BMI made its nadir during early childhood (5.6 and 4.9 years, respectively; Aronoff et al., 2022).

Literature tracking developmental trajectories of body compositions uncovers that fat mass underwent a nadir during early childhood (age 5 to 7), while lean mass had increased almost linearly (Plachta-Danielzik et al., 2013; Taylor et al., 2011). Integrating this evidence, Kuzawa and Blair (2019) propose that any variation in early brain energetics may influence overall energy balance, thereby modifying the trajectory and composition of weight gain and resulting in differential patterns of fat deposition. This insight might be partly supported by the observations of reduced volumes or cortical thickness in prefrontal regions (e.g., orbitofrontal cortex, superior frontal gyrus, inferior frontal gyrus), the ACC, amygdala, and hippocampus in relation to higher BMI or obesity in children and adolescents (Brooks et al., 2023; Jiang et al., 2023; Kim et al., 2020; Mestre et al., 2017). Nonetheless, this link between brain morphology and fat deposition might also be mediated by conditional neurophysiological processes, including excess adiposity-induced neuroinflammation or impaired insulin action in the central nervous system, which may in turn alter brain metabolism, synaptogenesis, and neuroplasticity (Boleti et al., 2022; Kullmann et al., 2016; Ly et al., 2023), suggesting an alternative direction of the brain-fat relationship.

Taken together, because of its highly prioritized energetics and profound connections with a variety of life functions, the developing brain could be responsive to variations in both internal neurophysiological processes and environmental condition and have implications for subsequent somatic development. Despite abundant work linking neurobiological alterations with excess adiposity, this brain-fat relationship was seldom investigated with the influences of environmental adversity, and the directionality of its pathway remains underexplored. To further comprehend the developmental covariation between brain morphology and body composition, there is a necessity to probe whether and how much, if any, environmentally induced variations in one energy-allocation target can be additionally explained by changes in the other. Therefore, using a large-scale youth sample from the Adolescent Brain Cognitive Development (ABCD®) Study, the current research aims to investigate how socioeconomic deprivation is longitudinally associated with variations in brain volumes and fat deposition pattern and whether the association of socioeconomic deprivation with one can be mediated by the other. We hypothesized total and regional brain volumes (e.g., the superior frontal gyrus, orbitofrontal cortex, ACC) to mediate the association between socioeconomic deprivation with increased later fat deposition; likewise, socioeconomic deprivation is associated with reduced brain volumes through the mediation of increased body fat.

2. Method

2.1. Sample

The present research used data from the ABCD® Study released by the National Institute of Mental Health Data Archive (NDA; ABCD® release 5.1, <https://abcdstudy.org>). The ABCD® Study is a large-scale study of child brain development and health, providing environmental, psychosocial, health, neuroimaging, and biospecimen data collected from approximately 12,000 8- to 11-year-old children and their caregivers across 21 research sites in the U.S. The central institutional review board (IRB) at the University of California, San Diego, accounted for ethical review and approval of protocol for most sites, with a few relying on local IRBs (Auchter et al., 2018). The current study is based on a sample of children with MRI scans across the baseline (T0; n = 11,782) and 2-year follow-up visits (T2; n = 8,092). This sample was further screened by 1) whether they ever had a traumatic brain injury or have been hospitalized due to head injury (n = 176) and 2) whether their age- and sex-corrected WHtR z values exceed ± 3 (n = 2). Participants who had a history of brain injury were dropped, and corrected BMI and WHtR beyond the z score cut-offs were replaced with NAs, giving rise to a final sample of 7,916. Demographic information of the final

Table 1
Demographic information of the final sample for analysis.

	n = 7,916	
	%	M (SD)
Child Age		9.46 (0.50)
Child Gender		
Male	53.78	
Female	46.21	
Child Race		
Non-Hispanic White	54.64	
Non-Hispanic Black	13.66	
Hispanic	19.25	
Asian	1.92	
Others	10.53	
Caregiver Age		39.94 (6.73)
Caregiver Gender		
Male	10.65	
Female	89.07	
Caregiver Race		
Non-Hispanic White	61.51	
Non-Hispanic Black	13.57	
Hispanic	11.11	
Asian	3.06	
Others	10.29	
Caregiver Education		16.67 (2.69)
> Master's	5.77	
Master's Degree	19.44	
Bachelor's Degree	29.08	
Associate Degree	13.08	
Some College or GED	18.72	
High School Graduate	7.77	
< High School	6.08	
Household Income		7.30 (2.32)
> \$200,000	10.08	
\$100,000 ~ \$199,999	28.40	
\$75,000 ~ \$99,999	14.17	
\$50,000 ~ \$74,999	13.35	
\$25,000 ~ \$49,999	13.77	
\$12,000 ~ \$24,999	6.32	
< \$12,000	6.13	

Note. Scales of caregiver's education attainment and household income were abbreviated for presentation. The original caregiver's education attainment is scaled with 21 bands, and so is household income with 10 bands, which were proceeded to analyses.

sample is shown in Table 1.

2.2. Measures

2.2.1. Socioeconomic deprivation (SED; T0)

Area deprivation index (ADI) is a composite measure of census-tract level socioeconomic status based on 17 factors, encompassing median household income, home value, gross rent, and monthly mortgage, income disparity, percentage of population aged 25 + years with at least a high school diploma or with less than 9 years of education, percentage of population aged 16 + years with a white-collar occupation or unemployed, and percentage of housing units below the poverty level or without utilities (e.g., motor vehicle, telephone plumbing; Fan et al., 2021; Knighton et al., 2016). The sum of the weighted 17 factors was standardized and adjusted to base mean of 100 with a standard deviation of 20. The ADI scores used in the present study were averaged scores across all reported residential addresses. A higher ADI score indicates a higher level of neighborhood disadvantage.

Needs-to-income ratio (NIR) was derived based on the 2017 federal poverty threshold per household size and number of related children under 18 years (<https://www.census.gov/data/tables/time-series/demo/income-poverty/historical-poverty-thresholds.html>) divided by the median value of the household-combined income band (10 bands in total). A higher NIR indicates a higher household financial requirement relative to the household's total income.

Material hardship (MH) was computed using caregiver reports on a 7-item questionnaire adapted from the measure for material hardship and deprivation by Diemer et al. (2013). This questionnaire assesses a family's unmet experiences of daily requirements for food, housing, utility, and medical care, etc. Caregivers were asked whether there has been a time their family has experienced a specific circumstance, such as "Needed food but couldn't afford to buy it or couldn't afford to go out to get it," "Had services turned off by the gas or electric company, or the oil company wouldn't deliver oil because payments were not made," "Had someone who needed to see a doctor or go to the hospital but didn't go because you could not afford it" and to respond with 1 = "Yes" or 0 = "No." Item scores were summed to derive a total score. The higher a total score, the more material shortages the family had experienced.

Caregiver education was obtained from participants' demographic information. Scores were reversed so that a higher score indicates higher educational disadvantage (Edu-R).

2.2.2. Waist-to-Height Ratio (WHtR; T0 & T2)

Waist-to-Height Ratio was computed based on the anthropometric records of stature and waist circumference. Calculated values were converted into z scores using the age- and sex-adjusted LMS parameters by Sharma et al. (2015) following the computation guide by WHO Multi-centre Growth Reference StudyGroup(2006).

2.2.3. Image acquisition & Structural variables (T0 & T2)

With the magnetic resonance imaging (MRI) protocol harmonized across 21 sites, 3 T MRI scanners (Siemens, Philips, and General Electric) equipped with a standard adult-size multi-channel coil were employed for imaging (Casey et al., 2018). Image processing and preliminary analysis were carried out by the ABCD® Data Analysis and Informatics Center for quality and consistency (Hagler et al., 2019). Structural images were corrected for head motions and non-linearity distortions. Cortical and subcortical reconstruction and segmentation were performed using FreeSurfer (Fischl, 2012) with labels of regions of interest (ROIs) assigned according to anatomically defined parcellations (Desikan et al., 2006; Destrieux et al., 2010; Fischl et al., 2002). Processed images were evaluated by trained professionals for quality. Derived morphometric measures encompass cortical thickness, sulcal depth, surface area, T1- and T2-weighted gray and white matter intensity and gray-to-white matter contrast, and cortical and subcortical volumes (Hagler et al., 2019). Measures were tabulated and complied in

files that were made publicly available by the NDA. According to the cortical ROI labeling by Desikan et al. (2006), the ROIs of the current study included the superior (SFG), middle (MFG), and inferior frontal gyrus (IFG), orbitofrontal cortex (OFC), frontal pole (FP), and anterior cingulate cortex (ACC) in both left and right hemispheres, total cortical volume (TCV), and total brain volume (TBV), with total intracranial volume (TIV) also involved for further processing.

2.2.4. Covariates

Pubertal status was derived using child reports on the Pubertal Development Scale (Carskadon & Acebo, 1993; Petersen et al., 1988). Children were asked to rate 1 = "Has not yet started" to 4 = "Seems complete" on 5 questions. Three questions regarding growth in height, body hair, and skin changes (e.g., pimple) were administered to both boys and girls. Beyond the three common questions, boys were inquired about changes in their voice and facial hair, while girls were asked about their breast growth and whether they have begun to menstruate. Following the algorithm by Petersen et al. (1988), scores on the body hair item and the two sex-specific items were converted into 5 developmental categories, coded as 1 = Prepubertal, 2 = Early Pubertal, 3 = Midpubertal, 4, Late Pubertal, 5 = Postpubertal, that a higher score indicates a maturer pubertal status.

Pubertal status, child age and sex at birth were specified as covariates for all analyses.

2.3. Statistical analyses

Statistical analyses were performed in R (v4.4.1; R Core Team, 2024). A bivariate Pearson's correlation analysis was conducted including all variables and covariates. Log transformation was applied to address right-skewness. To rule out variations in ROI volumes attributable to individual differences in head size, residual-based normalization was conducted by regressing each ROI volume on total intracranial volume and extracting the residuals for deriving normalized ROI volumes (Jack et al., 1989). Structural equation modeling (SEM) was performed using the lavaan package (Rosseel, 2012) to create a latent construct for SED based on the observed indicators ADI, NIR, MH, and Edu-R, with full information maximum likelihood estimation to handle missing data. Indicators were examined whether they significantly load to the latent construct ($p < 0.05$) and show a standardized loading > 0.30 (Hair et al., 2006). Goodness-of-fit statistics with a comparative fit index (CFI) ≥ 0.95 , a root mean squared error of approximation (RMSEA) ≤ 0.06 , and a standardized root mean square residual (SRMR) ≤ 0.08 indicate a good model fit (Hu & Bentler, 1999). The primary analysis consisted of two mediation models: with SED being the predictor variable for all models, the first model treated T0 ROI volumes as the mediator variable and T2 WHtR as the outcome variable (Fig. 1 Panel a), while the second model specified T0 WHtR as the mediator and T2 ROI volumes as the outcome variable (Fig. 1, Panel b). The two models were fitted for each ROI, with child age, sex at birth, and pubertal status controlled for. A bootstrapping analysis with 5,000 resamples was performed to estimate the mediating effect, p values, and 95 % confidence interval. False Discover Rate (FDR) correction (Benjamini & Hochberg, 1995) was applied to adjust for significance of effects. Effects with an FDR-adjusted p value < 0.025 (2 models for 2 hypotheses, 14 comparisons per model) and 95 % confidence interval excluding zero were considered statistically significant.

3. Results

3.1. Descriptive analyses

Demographic information of the final study sample is shown in Table 1. The results of the bivariate Pearson's correlation analysis are depicted in Fig. 2 with numeric results presented in Supplemental Table S1. The analysis showed that ADI, NIR, MH, and Edu-R were

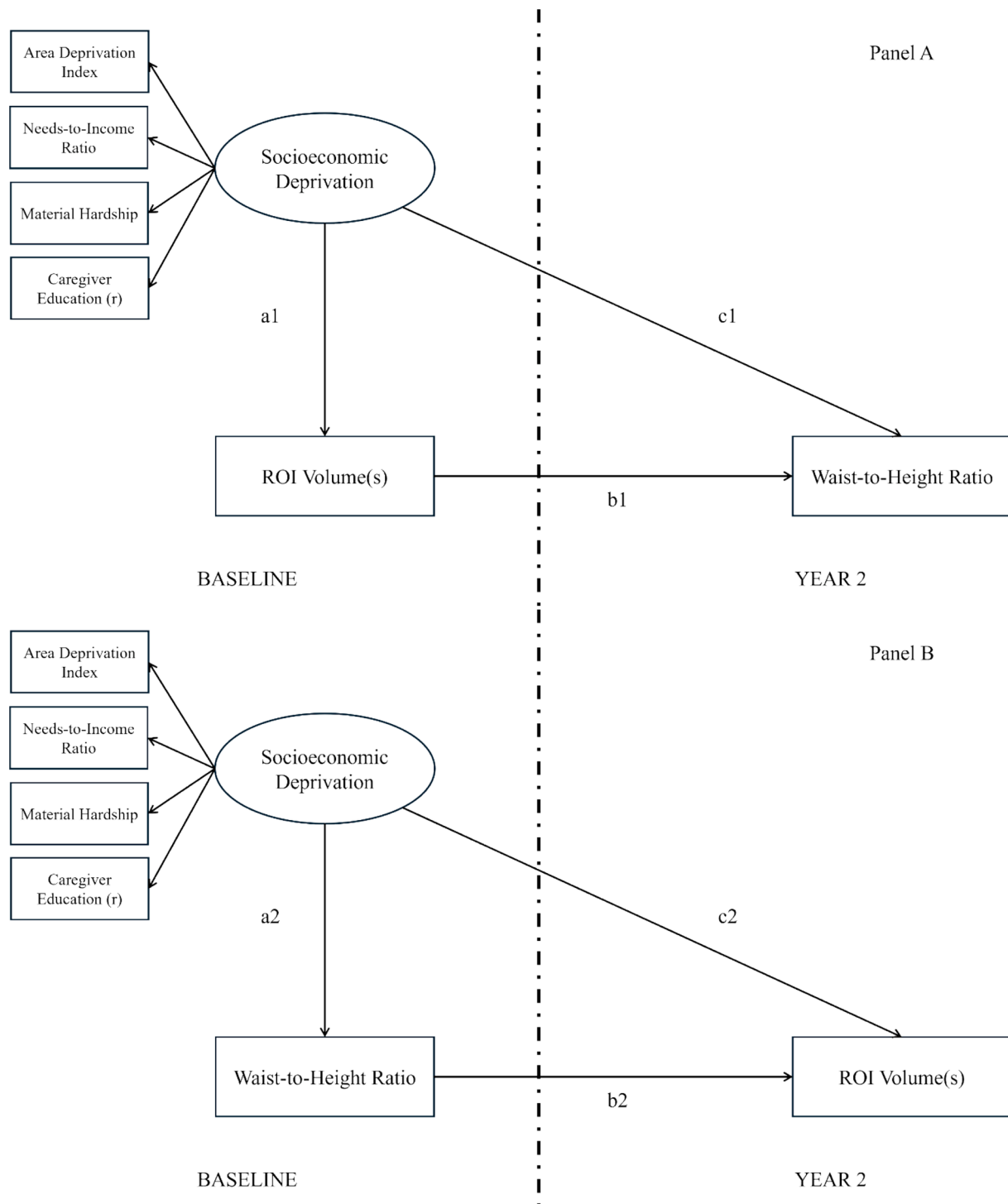


Fig. 1. Hypothetical Models with Distinct Structural Specifications across Times of Visit. *Note.* Panel A shows a model treating the volume of each brain region of interest (ROI) as the mediator variable and waist-to-height ratio (WHtR) as the outcome variable. Panel B displays a model setting WHtR as the mediator variable and volume in each brain ROI as the outcome variable. Variables on the left side of the dash line are based on baseline data, while the outcome variable on the right side is based on year-2 follow-up data.

positively correlated with WHtR and negatively with all (unnormalized) ROI volumes across all times of visit (p 's < 0.001). WHtR was negatively correlated with all ROI volumes at all times (p 's < 0.001, except for T0 right ACC, p 's < 0.01; T2 right ACC, p 's < 0.05; T0 WHtR and T2 TIV: $r = -0.039$, $p < 0.05$). In terms of covariates, age was not correlated with T0 WHtR but negatively with T2 WHtR at -0.023 ($p < 0.05$). Age was positively related with TIV and TBV and negatively with TCV at T0 and T2 (p 's < 0.05). For specific prefrontal regions, age was negatively

correlated to bilateral FP at (p 's < 0.001), and negatively with bilateral MFG, IFG, OFC, FP (p 's < 0.01), and the right ACC at T2 (p 's < 0.05). Sex at birth was negatively related to all ROI volumes at all times of visit (p 's < 0.001). PS was positively related with WHtR (p 's < 0.001) and negatively with all ROI volumes at all times of visit (p 's < 0.001, except for T0 TIV: $r = -0.026$, $p < 0.05$).

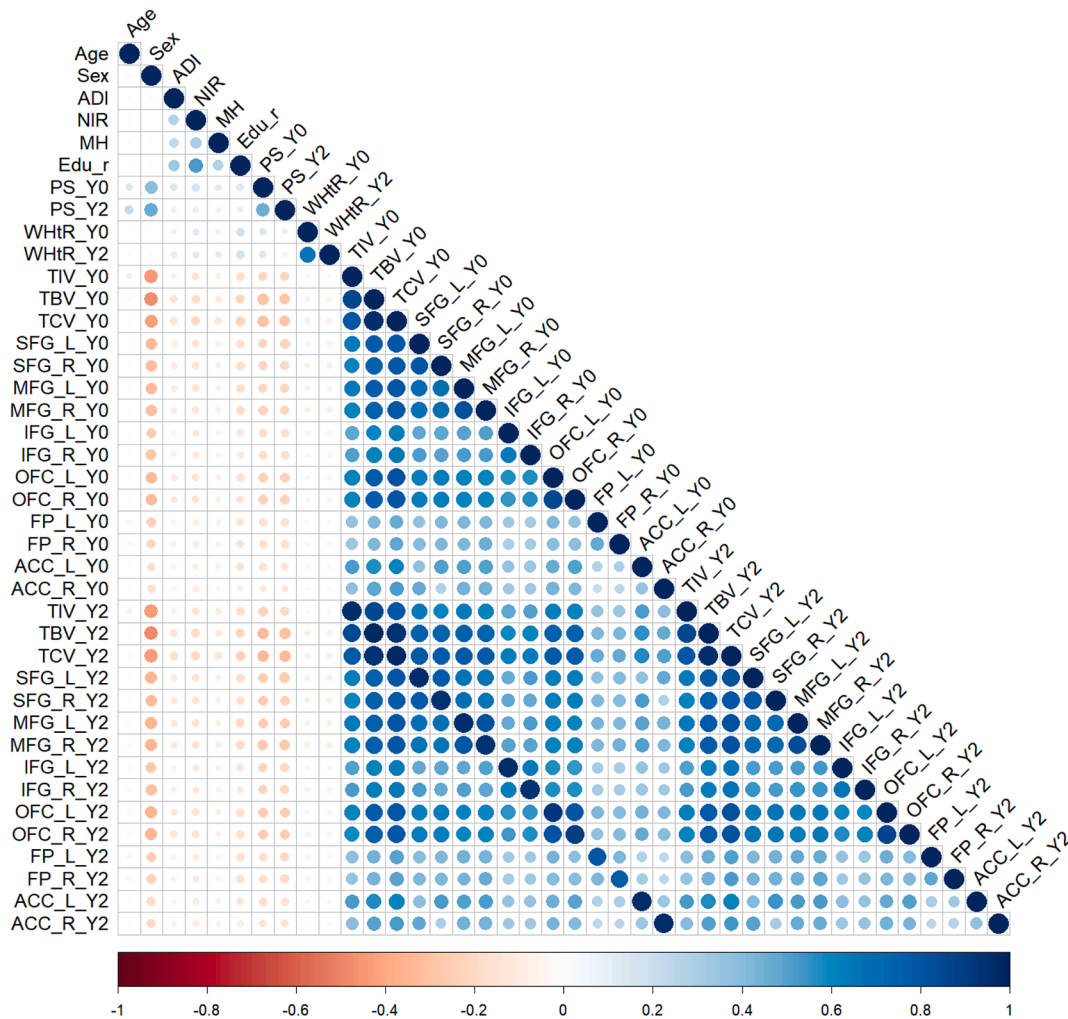


Fig. 2. Bivariate Correlation Between Main Variables of Interest and Covariates. Note. Y0/Y1, Baseline/Year-2 Follow-Up; ADI, Area Deprivation Index; NIR, Needs-to-Income Ratio; MH, Material Hardship; Edu_r, Caregiver Education Reversed; PS, Pubertal Status; WHtR, Waist-to-Height Ratio; TIV, Total Intracranial Volume; TBV, Total Brain Volume; TCV, Total Cortical Volume; L/R, Left/Right Hemisphere; SFG, Superior Frontal Gyrus; MFG, Middle Frontal Gyrus; IFG, Inferior Frontal Gyrus; OFC, Orbitofrontal Cortex; FP, Frontal Pole; ACC, Anterior Cingulate Cortex. Colors of circles toward darker blue indicate stronger positive correlations and darker red stronger negative correlations. Numeric results are shown in [Supplemental Table S1](#). (For interpretation of the references to colour in this figure legend, the reader is referred to the web version of this article.)

3.2. Primary mediation analyses

The measurement model for SED showed good fit: CFI = 0.999, RMSEA = 0.025, SRMR = 0.007. All indicators significantly loaded to the latent SED (p 's < 0.001): ADI = 0.575, NIR = 0.913, Edu-R = 0.675, MH = 0.492. Mediation analyses based on two models were fitted for normalized volumes in each ROI. Main results of mediation analyses are reported as follows:

3.2.1. Model 1: SED → baseline ROI Volumes → Year-2 WHtR

All mediation models testing whether ROI volumes mediate the relationship between SED and year-2 WHtR showed satisfactory fit: CFI > 0.956, RMSEA < 0.047, SRMR < 0.043 ([Supplemental Table S2](#)). Controlling for age, sex, and baseline PS, a higher SED was found to associate with reduced baseline volumes in all ROIs ($\beta_{TBV} = -0.174$, $\beta_{TCV} = -0.195$, $\beta_{PFC} = -0.060 \sim -0.115$, $\beta_{ACC} = -0.041 \sim -0.043$, FDR-adjusted p 's < 0.002) and with an increased WHtR at year-2 follow-up ($\beta = 0.185 \sim 0.194$, FDR-adjusted p 's < 0.001). With age, sex, and year-2 PS being controlled for, a reduced baseline TBV, TCV, a smaller bilateral SFG, MFG, and the right OFC was associated with a higher year-2 WHtR ($\beta_{TBV} = -0.040$, $\beta_{TCV} = -0.051$, $\beta_{PFC} = -0.037 \sim -0.060$, FDR-adjusted p 's < 0.003). Bilateral IFG, FP, ACC, and the left OFC did not

show a significant relationship with year-2 WHtR.

Bootstrapping analyses with 5,000 resamples indicated that TBV, TCV, and volumes in bilateral SFG, MFG, and the right OFC partially mediated the relationship between SED and year-2 WHtR ($\beta_{TBV} = 0.007$, $\beta_{TCV} = 0.010$, $\beta_{PFC} = 0.003 \sim 0.006$, FDR-adjusted p 's < 0.005). The volume in each of the seven identified ROIs accounted for 3.70 %, 5.05 %, 1.68 %, 2.69 %, 2.02 %, 3.03 %, and 2.02 % of the total effect, respectively (statistical results for unstandardized coefficients, standard errors, and 95 % CI are shown in [Table 2](#); for complete results including covariates see [Supplemental Table S3.1](#)).

3.2.2. Model 2: SED → baseline WHtR → Year-2 ROI volumes

All models testing the mediating effect of WHtR on the association of SED and year-2 ROI volumes fitted to data well: CFI > 0.955, RMSEA < 0.046, SRMR < 0.043 ([Supplemental Table S2](#)). With the covariates being identically controlled for, baseline SED showed an association with higher baseline WHtR ($\beta = 0.193 \sim 0.194$, FDR-adjusted p 's < 0.001) and with smaller volumes in all ROIs at year-2 ($\beta_{TBV} = -0.161$, $\beta_{TCV} = -0.179$, $\beta_{PFC} = -0.059 \sim -0.110$, $\beta_{ACC} = -0.040 \sim -0.042$, FDR-adjusted p 's < 0.003). A higher baseline WHtR was associated with a decreased TBV, TCV, and a reduced volume in bilateral SFG, MFG, FP, and the right IFG ($\beta_{TBV} = -0.037$, $\beta_{TCV} = -0.044$, $\beta_{PFC} = -0.030 \sim$

Table 2
Statistical result statistics of mediation analyses with primary variables of interest.

Models with baseline ROI volumes as the mediator variable and year-2 WHtR as the outcome variable								
DV	IV	Path	b	SE	p	95 % CI		β
TBV T0	SED	a1	−0.300	0.021	0.000	−0.341	−0.259	−0.174
WHtR T2	TBV T0	b1	−0.035	0.010	0.001	−0.055	−0.015	−0.040
	SED	c1	0.286	0.019	0.000	0.248	0.324	0.188
Indirect			0.011	0.003	0.001	0.004	0.017	0.007
Total			0.297	0.019	0.000	0.260	0.334	0.195
TCV T0	SED	a1	−0.336	0.021	0.000	−0.377	−0.295	−0.195
WHtR T2	TCV T0	b1	−0.045	0.010	0.000	−0.065	−0.025	−0.051
	SED	c1	0.282	0.019	0.000	0.244	0.320	0.185
Indirect			0.015	0.004	0.000	0.008	0.022	0.010
Total			0.297	0.019	0.000	0.260	0.334	0.195
SFG-L T0	SED	a1	−0.144	0.021	0.000	−0.185	−0.101	−0.083
WHtR T2	SFG-L T0	b1	−0.037	0.010	0.000	−0.056	−0.018	−0.042
	SED	c1	0.292	0.019	0.000	0.254	0.331	0.191
Indirect			0.005	0.002	0.001	0.002	0.009	0.003
Total			0.297	0.019	0.000	0.259	0.336	0.194
SFG-R T0	SED	a1	−0.196	0.021	0.000	−0.239	−0.153	−0.113
WHtR T2	SFG-R T0	b1	−0.041	0.010	0.000	−0.061	−0.022	−0.047
	SED	c1	0.289	0.019	0.000	0.250	0.326	0.189
Indirect			0.008	0.002	0.000	0.004	0.012	0.005
Total			0.297	0.019	0.000	0.258	0.334	0.194
MFG-L T0	SED	a1	−0.170	0.021	0.000	−0.212	−0.128	−0.098
WHtR T2	MFG-L T0	b1	−0.033	0.010	0.001	−0.052	−0.014	−0.037
	SED	c1	0.291	0.020	0.000	0.252	0.330	0.191
Indirect			0.006	0.002	0.002	0.002	0.009	0.004
Total			0.297	0.020	0.000	0.259	0.335	0.194
MFG-R T0	SED	a1	−0.171	0.022	0.000	−0.215	−0.130	−0.099
WHtR T2	MFG-R T0	b1	−0.053	0.010	0.000	−0.072	−0.034	−0.060
	SED	c1	0.288	0.020	0.000	0.250	0.328	0.189
Indirect			0.009	0.002	0.000	0.006	0.013	0.006
Total			0.297	0.020	0.000	0.259	0.337	0.195
IFG-L T0	SED	a1	−0.111	0.021	0.000	−0.153	−0.070	−0.064
WHtR T2	IFG-L T0	b1	−0.024	0.010	0.015	−0.044	−0.005	−0.028
	SED	c1	0.294	0.019	0.000	0.257	0.332	0.192
Indirect			0.003	0.001	0.027	0.001	0.005	0.002
Total			0.297	0.019	0.000	0.260	0.335	0.194
IFG-R T0	SED	a1	−0.103	0.022	0.000	−0.146	−0.061	−0.060
	IFG-R T0	b1	−0.021	0.010	0.032	−0.041	−0.002	−0.024
	SED	c1	0.294	0.019	0.000	0.258	0.332	0.193
Indirect			0.002	0.001	0.052	0.000	0.005	0.001
Total			0.297	0.019	0.000	0.260	0.334	0.194
OFC-L T0	SED	a1	−0.177	0.022	0.000	−0.219	−0.134	−0.102
WHtR T2	OFC-L T0	b1	−0.021	0.010	0.035	−0.040	−0.001	−0.024
	SED	c1	0.293	0.020	0.000	0.254	0.332	0.192
Indirect			0.004	0.002	0.039	0.000	0.007	0.002
Total			0.297	0.020	0.000	0.258	0.335	0.194
OFC-R T0	SED	a1	−0.189	0.021	0.000	−0.230	−0.148	−0.109
WHtR T2	MOFC-R T0	b1	−0.033	0.010	0.001	−0.052	−0.012	−0.037
	SED	c1	0.291	0.020	0.000	0.252	0.329	0.190
Indirect			0.006	0.002	0.002	0.002	0.010	0.004
Total			0.297	0.019	0.000	0.258	0.336	0.194
FP-L T0	SED	a1	−0.164	0.021	0.000	−0.206	−0.123	−0.095
WHtR T2	FP-L T0	b1	−0.008	0.010	0.407	−0.027	0.011	−0.009
	SED	c1	0.295	0.019	0.000	0.258	0.334	0.193
Indirect			0.001	0.002	0.414	−0.002	0.005	0.001
Total			0.297	0.019	0.000	0.259	0.335	0.194
FP-R T0	SED	a1	−0.199	0.021	0.000	−0.241	−0.158	−0.115
WHtR T2	FP-R T0	b1	−0.008	0.010	0.403	−0.028	0.011	−0.010
	SED	c1	0.295	0.020	0.000	0.258	0.333	0.193
Indirect			0.002	0.002	0.406	−0.002	0.006	0.001
Total			0.297	0.019	0.000	0.260	0.335	0.194
ACC-L T0	SED	a1	−0.074	0.021	0.000	−0.115	−0.033	−0.043
WHtR T2	ACC-L T0	b1	−0.019	0.010	0.054	−0.039	0.000	−0.021
	SED	c1	0.295	0.019	0.000	0.257	0.334	0.193
Indirect			0.001	0.001	0.097	0.000	0.003	0.001
Total			0.297	0.019	0.000	0.259	0.335	0.194
ACC-R T0	SED	a1	−0.072	0.022	0.001	−0.114	−0.028	−0.041
WHtR T2	ACC-R T0	b1	0.000	0.010	0.964	−0.019	0.019	0.000
	SED	c1	0.296	0.020	0.000	0.259	0.335	0.194
Indirect			0.000	0.001	0.965	−0.001	0.001	0.000
Total			0.297	0.019	0.000	0.259	0.335	0.194

Models with baseline WHtR as the mediator and year-2 ROI volumes as the outcome variable

(continued on next page)

Table 2 (continued)

Models with baseline ROI volumes as the mediator variable and year-2 WHtR as the outcome variable								
DV	IV	Path	b	SE	p	95 % CI		β
DV	IV	Path	b	SE	p	95 % CI		β
WHtR T0	SED	a2	0.299	0.019	0.000	0.261	0.337	0.194
TBV T2	WHtR T0	b2	−0.042	0.012	0.001	−0.066	−0.018	−0.037
	SED	c2	−0.279	0.021	0.000	−0.321	−0.237	−0.161
Indirect			−0.013	0.004	0.001	−0.020	−0.005	−0.007
Total			−0.292	0.021	0.000	−0.333	−0.251	−0.169
WHtR T0	SED	a2	0.299	0.019	0.000	0.261	0.337	0.194
TCV T2	WHtR T0	b2	−0.049	0.012	0.000	−0.073	−0.025	−0.044
	SED	c2	−0.308	0.021	0.000	−0.349	−0.267	−0.179
Indirect			−0.015	0.004	0.000	−0.022	−0.007	−0.008
Total			−0.323	0.021	0.000	−0.363	−0.282	−0.187
WHtR T0	SED	a2	0.299	0.020	0.000	0.261	0.338	0.194
SFG-L T2	WHtR T0	b2	−0.044	0.013	0.001	−0.069	−0.019	−0.040
	SED	c2	−0.125	0.022	0.000	−0.168	−0.082	−0.072
Indirect			−0.013	0.004	0.001	−0.021	−0.006	−0.008
Total			−0.138	0.022	0.000	−0.181	−0.096	−0.080
WHtR T0	SED	a2	0.299	0.020	0.000	0.260	0.339	0.194
SFG-R T2	WHtR T0	b2	−0.064	0.013	0.000	−0.089	−0.038	−0.057
	SED	c2	−0.164	0.022	0.000	−0.207	−0.121	−0.094
Indirect			−0.019	0.004	0.000	−0.027	−0.011	−0.011
Total			−0.183	0.021	0.000	−0.225	−0.141	−0.105
WHtR T0	SED	a2	0.299	0.020	0.000	0.261	0.339	0.194
MFG-L T2	WHtR T0	b2	−0.062	0.013	0.000	−0.086	−0.037	−0.055
	SED	c2	−0.156	0.022	0.000	−0.197	−0.113	−0.090
Indirect			−0.018	0.004	0.000	−0.026	−0.011	−0.011
Total			−0.174	0.021	0.000	−0.215	−0.133	−0.100
WHtR T0	SED	a2	0.299	0.020	0.000	0.262	0.339	0.194
MFG-R T2	WHtR T0	b2	−0.069	0.013	0.000	−0.094	−0.045	−0.062
	SED	c2	−0.145	0.022	0.000	−0.188	−0.103	−0.084
Indirect			−0.021	0.004	0.000	−0.029	−0.013	−0.012
Total			−0.166	0.021	0.000	−0.208	−0.125	−0.096
WHtR T0	SED	a2	0.299	0.020	0.000	0.261	0.337	0.193
IFG-L T2	WHtR T0	b2	−0.015	0.013	0.241	−0.040	0.009	−0.013
	SED	c2	−0.103	0.021	0.000	−0.146	−0.062	−0.060
Indirect			−0.004	0.004	0.243	−0.012	0.003	−0.003
Total			−0.108	0.021	0.000	−0.150	−0.067	−0.062
WHtR T0	SED	a2	0.299	0.020	0.000	0.262	0.339	0.193
IFG-R T2	WHtR T0	b2	−0.033	0.012	0.007	−0.058	−0.010	−0.030
	SED	c2	−0.103	0.022	0.000	−0.146	−0.060	−0.059
Indirect			−0.010	0.004	0.008	−0.018	−0.003	−0.006
Total			−0.113	0.021	0.000	−0.155	−0.071	−0.065
WHtR T0	SED	a2	0.299	0.020	0.000	0.261	0.338	0.194
OFC-L T2	WHtR T0	b2	−0.007	0.013	0.598	−0.031	0.019	−0.006
	SED	c2	−0.167	0.022	0.000	−0.211	−0.126	−0.096
Indirect			−0.002	0.004	0.598	−0.009	0.006	−0.001
Total			−0.169	0.021	0.000	−0.211	−0.129	−0.097
WHtR T0	SED	a2	0.299	0.020	0.000	0.262	0.338	0.194
OFC-R T2	WHtR T0	b2	−0.024	0.013	0.058	−0.049	0.001	−0.021
	SED	c2	−0.191	0.022	0.000	−0.233	−0.150	−0.110
Indirect			−0.007	0.004	0.060	−0.015	0.000	−0.004
Total			−0.198	0.021	0.000	−0.239	−0.157	−0.114
WHtR T0	SED	a2	0.299	0.019	0.000	0.262	0.338	0.194
FP-L T2	WHtR T0	b2	−0.049	0.013	0.000	−0.074	−0.024	−0.043
	SED	c2	−0.124	0.021	0.000	−0.167	−0.082	−0.071
Indirect			−0.015	0.004	0.000	−0.023	−0.007	−0.008
Total			−0.139	0.021	0.000	−0.180	−0.097	−0.080
WHtR T0	SED	a2	0.299	0.020	0.000	0.261	0.339	0.194
FP-R T2	WHtR T0	b2	−0.040	0.013	0.002	−0.065	−0.015	−0.035
	SED	c2	−0.173	0.022	0.000	−0.216	−0.130	−0.099
Indirect			−0.012	0.004	0.003	−0.020	−0.004	−0.007
Total			−0.184	0.021	0.000	−0.227	−0.143	−0.106
WHtR T0	SED	a2	0.299	0.020	0.000	0.261	0.339	0.193
ACC-L T2	WHtR T0	b2	−0.024	0.013	0.066	−0.048	0.002	−0.021
	SED	c2	−0.073	0.021	0.001	−0.115	−0.032	−0.042
Indirect			−0.007	0.004	0.067	−0.015	0.001	−0.004
Total			−0.080	0.021	0.000	−0.121	−0.040	−0.046
WHtR T0	SED	a2	0.299	0.019	0.000	0.262	0.337	0.193
ACC-R T2	WHtR T0	b2	0.003	0.013	0.839	−0.022	0.028	0.002
	SED	c2	−0.070	0.022	0.002	−0.113	−0.026	−0.040
Indirect			0.001	0.004	0.839	−0.007	0.008	0.000
Total			−0.069	0.022	0.001	−0.112	−0.026	−0.040

Note. T0/T2, Baseline/Year-2 Follow-Up; SED, Socioeconomic Deprivation; WHtR, Waist-to-Height Ratio; TBV, Total Brain Volume; TCV, Total Cortical Volume; -L/-R, Left/Right Hemisphere; SFG, Superior Frontal Gyrus; MFG, Middle Frontal Gyrus; IFG, Inferior Frontal Gyrus; OFC, Orbitofrontal Cortex; FP, Frontal Pole; ACC, Anterior Cingulate Cortex; Indirect, Indirect Effect; Total, Total Effect.

Path notes (a, b, and c) correspond to panels displayed in Fig. 1 Panel A and B. Unstandardized (b) and standardized coefficients (β), standard errors (SE), p values, and 95% confidence intervals of indirect effects were estimated based on bootstrapping analysis with 5,000 resamples. Regression statistics of all brain regional volumes tested with covariates are presented in Supplemental Table S3.

-0.062 , FDR-adjusted p 's < 0.012). No statistically significant effects were found with bilateral IFG, OFC, or ACC.

Bootstrapping analyses with the same setting showed that baseline WHtR partially mediated the relationship of SED with TBV, TCV, and volumes in bilateral SFG, MFG, FP, and the right IFG at year-2 ($\beta_{TBV} = -0.007$, $\beta_{TCV} = -0.008$, $\beta_{PFC} = -0.006 \sim -0.012$, FDR-adjusted $p < 0.012$), explaining 4.45 %, 4.64 %, 9.42 %, 10.38 %, 10.34 %, 12.65 %, 7.52 %, 10.79 %, and 6.52 % of the total effect, respectively (Table 2; complete statistical results in Supplemental Table S3.2).

4. Discussion

With mediation analyses performed to examine the relationships between SED, WHtR, and each ROI volume, several intriguing findings emerged. As hypothesized, SED was found to longitudinally associate with higher WHtR through the mediation of a reduced TBV, TCV, volume in bilateral SFG, MFG, and the right OFC; WHtR mediated the longitudinal relationship of SED with a smaller TBV, TCV, SFG, MFG, FP, and right IFG. Each of the findings is discussed in detail as follows.

In line with previous work (e.g., Hanson et al., 2013; McDermott et al., 2019; Taylor et al., 2020; Yang et al., 2016), socioeconomic deprivation showed cross-sectional and longitudinal associations with reduced volumes in whole brain, the cerebral cortex, all prefrontal regions, and the ACC. This finding lends support to models predicting environmental deprivation to alter early neural functioning (e.g., synaptogenesis, pruning) by disturbing environmental inputs to the brain, resulting in atypical neural organizations (McLaughlin et al., 2014, 2019; Sheridan & McLaughlin, 2014). More recent models suggest that socioeconomic status (SES), in particular, affects the pace and trajectory of neural development during childhood and adolescence (Rakesh et al., 2023; Rakesh & Whittle, 2021). Based on an extensive review of longitudinal evidence, the authors conclude that children from lower SES backgrounds may experience delayed, attenuated neural developmental trajectories, characterized by consistently smaller increases and lower peaks in cortical and subcortical structures relative to their high-SES peers (Rakesh et al., 2023). Our findings add to these observations of attenuated neural development by exhibiting consistent reductions in both global and regional neural structures as a function of socioeconomic deprivation.

Our mediation analyses indicate that socioeconomic deprivation shaped later fat deposition pattern through the mediation of reduced brain structures. This finding may suggest a possibility that as a result of environmental deprivation, altered neural development – manifest as smaller structures than expected at each timepoint and/or a generally lower maximum size – may reflect an energy-allocation strategy favoring less investment in the brain for the sake of development of traits or functions more adaptive to immediate environmental challenges. One preferred energy-allocation target seems to be adipose tissue, which serves as common energy currency for financing development of other age-specific functions (e.g., maturation, as presented in Supplemental Table S3 that pubertal status was consistently negatively related to brain volumes and positively with WHtR; Wells, 2023). One example lies in a shared observation in the LH literature aforementioned: while the inverse relationship between immune response and growth in height was evident in children with lower body fat (measured by skinfold thickness), it was not observed in children with higher body fat, suggesting a potential role of body fat in relaxing this trade-off (McDade et al., 2008; Shattuck-Heidorn et al., 2017; Urlacher et al., 2018). In this sense, increased fat deposition may be adaptively accompanied with attenuated brain development, formulating a suite of inversely correlated phenotypic traits (i.e., trade-off) favoring maintenance over growth under environmental deprivation, as predicted by Ellis et al. (2022).

This interpretation is largely based on the LH concept of *embodied capitals*, which refer to organisms' externalizing physical properties and functions of energy-allocation strategies for ultimate reproductive success (Del Giudice et al., 2015). Nevertheless, whether, or how much, if any, this brain-fat link is mediated by brain energetics as proposed by Kuzawa and Blair's (2019) is not reflected in the current research and therefore remains an open question pending for further research based on more direct measures.

Moreover, in line with a previous study using the same baseline sample (Dennis et al., 2022), our analyses also demonstrated that socioeconomic deprivation was longitudinally associated with reduced brain volumes through increased fat deposition. This pattern suggests that environmental deprivation may alter brain morphology both through a direct, extrinsic effect and via an internally mediated effect on the brain. Neurobiological alterations associated with excess adiposity may be attributable to elevated pro-inflammatory cytokines (e.g., TNF- α , IL-6) and adipokines (e.g., leptin), which may compromise blood–brain barrier integrity and over-activate microglia, astrocytes, and other cells, ultimately contributing to central inflammation and subsequent structural atrophy (Boleti et al., 2022; Ly et al., 2023). Relevant to these processes is insulin resistance, which could be due to downregulation of insulin receptors (abundant in the PFC, hippocampus and hypothalamus) triggered by hyperinsulinemia and neuroinflammation (Cui et al., 2022; Kullmann et al., 2016). Notably, when comparing results of all analyses, fat deposition appeared to be consistently associated with specific prefrontal structures (bilateral SFG and MFG), which may suggest a bidirectional brain-fat pathway, but differentially with others depending on the directionality of its relationship with them. Environmentally-induced or fat-mediated alterations in brain structures related to inhibitory control (e.g., the SFG, MFG, and IFG; Batterink et al., 2010; Kim et al., 2020; Lavagnino et al., 2016) and food reward and appetite (e.g., the OFC; Maayan et al., 2011; for a review see Dagher, 2012) may imply a potential effect of eating pattern within the brain-fat association. This effect could be particularly associated with socioeconomic disadvantages due to socio-geographical disparities in food environment and diet quality (Mölenberg et al., 2021; Zarnowiecki et al., 2014).

The current research is subject to several limitations. First, our use of anthropometric measure to indicate body fat must be treated with scrutiny. With BMI being one of the most widely used surrogate measure of body fat, however, this weight-based measure could be confounded with lean mass, especially in developing populations whose body fat might experience a rebound while their lean mass escalates almost linearly (Plachta-Danielzik et al., 2013; Taylor et al., 2011). To address this potential bias, we used age- and sex-adjusted WHtR instead, yet the central issue remains – excess adiposity might be more accurately captured by higher percentiles of the measure but likely confounded within the lower. Therefore, we stress the necessity of using more direct or integrated measures of adipose tissue (e.g., fat mass index, body fat percentage) in future research. Second, excess adiposity is a function of a wide range of factors, such as genetic predispositions, metabolic complications, developmental shifts of hormones, physical activity, and perhaps most pronouncedly, dietary habit and nutrition intake. Based on our observed differential reductions in prefrontal structures, we suspect that the brain-fat pathway may be partially explained by food intake pattern, which was not tested in the current research and would thus constrain the interpretability of our results. Third, the peak of total/cortical gray matter volume varies greatly by sex and brain region and widely during childhood through early adolescence (Bethlehem et al., 2022; Schabdach et al., 2023). In addition to our observation that age was consistently negatively associated with brain volumes (Supplemental Table S3), we conducted an exploratory paired-samples t -

test and found that total cortical volume at year-2 was significantly lower than its baseline volume ($t = 73.37(7,849)$, $p < 0.001$, Cohen's $d = 0.195$), suggesting that our sample might be undergoing an age-related decline in gray matter volume. Although age was controlled for in testing associations, this age-specific structural variation might incur additional difficulty for interpreting our results, and we thereby claim this as a limitation.

In conclusion, global brain structures (e.g., whole brain volume, total cortical volume) were longitudinally negatively associated with fat deposition in addition to the impact of socioeconomic deprivation, whereas prefrontal regions exhibited nuanced relationships. From an LH perspective, the longitudinal coupling of increased fat deposition and reductions in neural structures may reflect a functional trade-off strategy for environmental adversity. Although future studies with more direct, targeted measures are needed, these findings have implications for the understanding of neural and somatic development in children and adolescents across diverse socioeconomic contexts.

Ethics Approval

The ABCD research sites are subject to the ethical review and approval by the central Institutional Review Board (IRB) at the University of California, San Diego, and IRBs at local institutions.

Consent to publish

Informed consent to publish was not necessary because all data used for the present research came from the National Institute of Mental Health Data Archive.

Use of generative AI

No generative AI products or AI-integrated tools were used during the development of the current research.

CRedit authorship contribution statement

Anting Yang: Writing – original draft, Visualization, Software, Methodology, Investigation, Formal analysis, Data curation, Conceptualization. **Hui Jing Lu:** Writing – review & editing, Visualization, Validation, Supervision, Software, Methodology, Investigation, Formal analysis, Data curation, Conceptualization. **Lei Chang:** Writing – review & editing, Writing – original draft, Validation, Supervision, Resources, Project administration, Methodology, Investigation, Formal analysis, Conceptualization.

Funding

The authors declare that no funds, grants, or other supports were received during the development of this manuscript.

Declaration of competing interest

The authors declare that they have no known competing financial interests or personal relationships that could have appeared to influence the work reported in this paper.

Acknowledgements

Data used in the preparation of this article were obtained from the Adolescent Brain Cognitive Development (ABCD) Study (<https://abcdstudy.org>), held in the NIMH Data Archive (NDA). This is a multi-site, longitudinal study designed to recruit more than 10,000 children age 9–10 and follow them over 10 years into early adulthood. The ABCD Study® is supported by the National Institutes of Health and additional federal partners under award numbers U01DA041048, U01DA050989,

U01DA051016, U01DA041022, U01DA051018, U01DA051037, U01DA050987, U01DA041174, U01DA041106, U01DA041117, U01DA041028, U01DA041134, U01DA050988, U01DA051039, U01DA041156, U01DA041025, U01DA041120, U01DA051038, U01DA041148, U01DA041093, U01DA041089, U24DA041123, U24DA041147. A full list of supporters is available at <https://abcdstudy.org/federal-partners.html>. A listing of participating sites and a complete listing of the study investigators can be found at https://abcdstudy.org/consortium_members/. ABCD consortium investigators designed and implemented the study and/or provided data but did not necessarily participate in the analysis or writing of this report. This manuscript reflects the views of the authors and may not reflect the opinions or views of the NIH or ABCD consortium investigators.

Appendix A. Supplementary material

Supplementary data to this article can be found online at <https://doi.org/10.1016/j.bandc.2025.106315>.

Data availability

Data Availability: The ABCD data repository grows and changes over time. The data used in this report is available upon application and can be found at <https://doi.org/10.15154/z563-zd24>.

References

- Aronoff, J. E., Ragin, A., Wu, C., Markl, M., Schnell, S., Shaibani, A., Blair, C., & Kuzawa, C. W. (2022). Why do humans undergo an adiposity rebound? Exploring links with the energetic costs of brain development in childhood using MRI-based 4D measures of total cerebral blood flow. *International Journal of Obesity*, 46(5), 1044–1050. <https://doi.org/10.1038/s41366-022-01065-8>
- Auchter, A. M., Hernandez Mejia, M., Heyser, C. J., Shilling, P. D., Jernigan, T. L., Brown, S. A., Tapert, S. F., & Dowling, G. J. (2018). A description of the ABCD organizational structure and communication framework. *Developmental Cognitive Neuroscience*, 32, 8–15. <https://doi.org/10.1016/j.dcn.2018.04.003>
- Batterink, L., Yokum, S., & Stice, E. (2010). Body mass correlates inversely with inhibitory control in response to food among adolescent girls: An fMRI study. *NeuroImage*, 52(4), 1696–1703. <https://doi.org/10.1016/j.neuroimage.2010.05.059>
- Benjamini, Y., & Hochberg, Y. (1995). Controlling the false discovery rate: A practical and powerful approach to multiple testing. *Journal of the Royal Statistical Society: Series B (Methodological)*, 57(1), 289–300. <https://doi.org/10.1111/j.2517-6161.1995.tb02031.x>
- Bethlehem, R. a. I., Seidlitz, J., White, S. R., Vogel, J. W., Anderson, K. M., Adamson, C., Adler, S., Alexopoulos, G. S., Anagnostou, E., Arcese-Gonzalez, A., Astle, D. E., Auyeung, B., Ayub, M., Bae, J., Ball, G., Baron-Cohen, S., Beare, R., Bedford, S. A., Benegal, V., ... Alexander-Bloch, A. F. (2022). Brain charts for the human lifespan. *Nature*, 604(7906), 525–533. <https://doi.org/10.1038/s41586-022-04554-y>
- Bogin, B., Silva, M. I. V., & Rios, L. (2007). Life history trade-offs in human growth: Adaptation or pathology? *American Journal of Human Biology*, 19(5), 5. <https://doi.org/10.1002/ajhb.20666>
- Boleti, A. P. de A., Cardoso, P. H. de O., Frihling, B. E. F., Silva, P. S. e, Moraes, L. F. R. N. de, & Migliolo, L. (2022). Adipose tissue, systematic inflammation, and neurodegenerative diseases. *Neural Regeneration Research*, 18(1), 38–46. <https://doi.org/10.4103/1673-5374.343891>
- Brooks, S. J., Smith, C., & Stamoulis, C. (2023). Excess BMI in early adolescence adversely impacts maturing functional circuits supporting high-level cognition and their structural correlates. *International Journal of Obesity*, 47(7), 590–605. <https://doi.org/10.1038/s41366-023-01303-7>
- Carskadon, M. A., & Acebo, C. (1993). A self-administered rating scale for pubertal development. *Journal of Adolescent Health*, 14(3), 190–195. [https://doi.org/10.1016/1054-139X\(93\)90004-9](https://doi.org/10.1016/1054-139X(93)90004-9)
- Casey, B. J., Cannonier, T., Conley, M. I., Cohen, A. O., Barch, D. M., Heitzeg, M. M., Soules, M. E., Teslovich, T., Dellarco, D. V., Garavan, H., Orr, C. A., Wager, T. D., Banich, M. T., Speer, N. K., Sutherland, M. T., Riedel, M. C., Dick, A. S., Bjork, J. M., Thomas, K. M., & Dale, A. M. (2018). The adolescent brain cognitive development (ABCD) study: Imaging acquisition across 21 sites. *Developmental Cognitive Neuroscience*, 32, 43–54. <https://doi.org/10.1016/j.dcn.2018.03.001>
- Cui, Y., Tang, T.-Y., Lu, C.-Q., & Ju, S. (2022). Insulin resistance and cognitive impairment: Evidence from neuroimaging. *Journal of Magnetic Resonance Imaging*, 56(6), 1621–1649. <https://doi.org/10.1002/jmri.28358>
- Dagher, A. (2012). Functional brain imaging of appetite. *Trends in Endocrinology & Metabolism*, 23(5), 250–260. <https://doi.org/10.1016/j.tem.2012.02.009>
- Del Giudice, M., Gangestad, S. W., & Kaplan, S. (2015). Life history theory and evolutionary psychology. In D. M. Buss (Ed.), *The Handbook of Evolutionary Psychology: Vol. Foundations* (2nd ed., pp. 88–114). John Wiley & Sons, Inc.

- Dennis, E., Manza, P., & Volkow, N. D. (2022). Socioeconomic status, BMI, and brain development in children. *Translational Psychiatry*, 12(1). <https://doi.org/10.1038/s41398-022-01779-3>. Article 1.
- Desikan, R. S., Ségonne, F., Fischl, B., Quinn, B. T., Dickerson, B. C., Blacker, D., Buckner, R. L., Dale, A. M., Maguire, R. P., Hyman, B. T., Albert, M. S., & Killiany, R. J. (2006). An automated labeling system for subdividing the human cerebral cortex on MRI scans into gyral based regions of interest. *NeuroImage*, 31(3), 968–980. <https://doi.org/10.1016/j.neuroimage.2006.01.021>
- Destrieux, C., Fischl, B., Dale, A., & Halgren, E. (2010). Automatic parcellation of human cortical gyri and sulci using standard anatomical nomenclature. *NeuroImage*, 53(1), 1–15. <https://doi.org/10.1016/j.neuroimage.2010.06.010>
- Diemer, M. A., Mistry, R. S., Wadsworth, M. E., López, L., & Reimers, F. (2013). Best practices in conceptualizing and measuring social class in psychological research. *Analyses of Social Classes and Public Policy*, 13(1), 77–113. <https://doi.org/10.1111/asap.12001>
- Ellis, B. J., Figueredo, A. J., Brumbach, B. H., & Schlomer, G. L. (2009). Fundamental dimensions of environmental risk: The impact of harsh versus unpredictable environments on the evolution and development of life history strategies. *Human Nature*, 20(2). <https://doi.org/10.1007/s12110-009-9063-7>. Article 2.
- Ellis, B. J., Sheridan, M. A., Belsky, J., & McLaughlin, K. A. (2022). Why and how does early adversity influence development? Toward an integrated model of dimensions of environmental experience. *Development and Psychopathology*, 34(2), 447–471. <https://doi.org/10.1017/S0954579421001838>
- Fan, C. C., Marshall, A., Smolker, H., Gonzalez, M. R., Tapert, S. F., Barch, D. M., Sowell, E., Dowling, G. J., Cardenas-Iniguez, C., Ross, J., Thompson, W. K., & Herting, M. M. (2021). Adolescent Brain Cognitive Development (ABCD) study Linked External Data (LED): Protocol and practices for geocoding and assignment of environmental data. *Developmental Cognitive Neuroscience*, 52, Article 101030. <https://doi.org/10.1016/j.dcn.2021.101030>
- Fischl, B. (2012). FreeSurfer. *NeuroImage*, 62(2), 774–781. <https://doi.org/10.1016/j.neuroimage.2012.01.021>
- Fischl, B., Salat, D. H., Busa, E., Albert, M., Dieterich, M., Haselgrove, C., van der Kouwe, A., Killiany, R., Kennedy, D., Klaveness, S., Montillo, A., Makris, N., Rosen, B., & Dale, A. M. (2002). Whole brain segmentation: Automated labeling of neuroanatomical structures in the human brain. *Neuron*, 33(3), 341–355. [https://doi.org/10.1016/S0896-6273\(02\)00569-X](https://doi.org/10.1016/S0896-6273(02)00569-X)
- Fonseca-Azevedo, K., & Herculano-Houzel, S. (2012). Metabolic constraint imposes tradeoff between body size and number of brain neurons in human evolution. *Proceedings of the National Academy of Sciences of the United States of America*, 109(45), 18571–18576. <https://doi.org/10.1073/pnas.1206390109>
- Geary, D. C. (2003). Sexual selection and human life history. In R. V. Kail (Ed.), *Advances in Child Development and Behavior* (Vol. 30, pp. 41–101). JAI. [https://doi.org/10.1016/S0065-2407\(02\)80039-8](https://doi.org/10.1016/S0065-2407(02)80039-8)
- Hagler, D. J., Hatton, S. N., Cornejo, M. D., Makowski, C., Fair, D. A., Dick, A. S., Sutherland, M. T., Casey, B. J., Barch, D. M., Harms, M. P., Watts, R., Bjork, J. M., Garavan, H. P., Hilmer, L., Pung, C. J., Scat, C. S., Kuperman, J., Bartsch, H., Xue, F., & Dale, A. M. (2019). Image processing and analysis methods for the Adolescent Brain Cognitive Development Study. *NeuroImage*, 202, Article 116091. <https://doi.org/10.1016/j.neuroimage.2019.116091>
- Hair, J. F., Black, W. C., Babin, B. J., Anderson, R. E., & Tatham, R. L. (2006). *Multivariate data analysis*. Pearson.
- Hanson, J. L., Hair, N., Shen, D. G., Shi, F., Gilmore, J. H., Wolfe, B. L., & Pollak, S. D. (2013). Family poverty affects the rate of human infant brain growth. *PLoS One*, 8(12), Article e80954. <https://doi.org/10.1371/journal.pone.0080954>
- Herculano-Houzel, S. (2012). The remarkable, yet not extraordinary, human brain as a scaled-up primate brain and its associated cost. *Proceedings of the National Academy of Sciences*, 109(supplement_1), 10661–10668. <https://doi.org/10.1073/pnas.1201895109>
- Hu, L., & Bentler, P. M. (1999). Cutoff criteria for fit indexes in covariance structure analysis: Conventional criteria versus new alternatives. *Structural Equation Modeling: A Multidisciplinary Journal*, 6(1), 1–55. <https://doi.org/10.1080/10705519909540118>
- Isler, K., & van Schaik, C. P. (2009). The expensive brain: A framework for explaining evolutionary changes in brain size. *Journal of Human Evolution*, 57(4), 392–400. <https://doi.org/10.1016/j.jhevol.2009.04.009>
- Jack, C. R., Twomey, C. K., Zinsmeister, A. R., Sharbrough, F. W., Petersen, R. C., & Cascino, G. D. (1989). Anterior temporal lobes and hippocampal formations: Normative volumetric measurements from MR images in young adults. *Radiology*, 172(2), 549–554. <https://doi.org/10.1148/radiology.172.2.2748838>
- Jiang, F., Li, G., Ji, W., Zhang, Y., Wu, F., Hu, Y., Zhang, W., Manza, P., Tomasi, D., Volkow, N. D., Gao, X., Wang, G.-J., & Zhang, Y. (2023). Obesity is associated with decreased gray matter volume in children: A longitudinal study. *Cerebral Cortex*, 33(7), 3674–3682. <https://doi.org/10.1093/cercor/bhac300>
- Kim, M. S., Luo, S., Azad, A., Campbell, C. E., Felix, K., Cabeen, R. P., Belcher, B. R., Kim, R., Serrano-Gonzalez, M., & Herting, M. M. (2020). Prefrontal cortex and amygdala subregion morphology are associated with obesity and dietary self-control in children and adolescents. *Frontiers in Human Neuroscience*, 14. <https://doi.org/10.3389/fnhum.2020.563415>
- Knighton, A. J., Savitz, L., Belnap, T., Stephenson, B., & VanDerslice, J. (2016). Introduction of an Area Deprivation Index measuring patient socioeconomic status in an integrated health system: Implications for population health. *eGEMS*, 4(3). <https://doi.org/10.13063/2327-9214.1238>. Article 3.
- Kullmann, S., Heni, M., Hallschmid, M., Fritsche, A., Preissl, H., & Häring, H.-U. (2016). Brain insulin resistance at the crossroads of metabolic and cognitive disorders in humans. *Physiological Reviews*, 96(4), 1169–1209. <https://doi.org/10.1152/physrev.00032.2015>
- Kuzawa, C. W., & Blair, C. (2019). A hypothesis linking the energy demand of the brain to obesity risk. *Proceedings of the National Academy of Sciences*, 116(27), 13266–13275. <https://doi.org/10.1073/pnas.1816908116>
- Kuzawa, C. W., Chugani, H. T., Grossman, L. I., Lipovich, L., Muzik, O., Hof, P. R., Wildman, D. E., Sherwood, C. C., Leonard, W. R., & Lange, N. (2014). Metabolic costs and evolutionary implications of human brain development. *Proceedings of the National Academy of Sciences*, 111(36), Article 36. <https://doi.org/10.1073/pnas.1323099111>
- Lavagnino, L., Mwangi, B., Bauer, I. E., Cao, B., Selvaraj, S., Prossin, A., & Soares, J. C. (2016). Reduced inhibitory control mediates the relationship between cortical thickness in the right superior frontal gyrus and body mass index. *Neuropsychopharmacology*, 41(9), 2275–2282. <https://doi.org/10.1038/npp.2016.26>
- Lawson, G. M., Duda, J. T., Avants, B. B., Wu, J., & Farah, M. J. (2013). Associations between children's socioeconomic status and prefrontal cortical thickness. *Developmental Science*, 16(5), 641–652. <https://doi.org/10.1111/desc.12096>
- Ly, M., Yu, G. Z., Mian, A., Cramer, A., Meysami, S., Merrill, D. A., Samara, A., Eisenstein, S. A., Hershey, T., Babulal, G. M., Lenze, E. J., Morris, J. C., Benzinger, T. L. S., & Raji, C. A. (2023). Neuroinflammation: A modifiable pathway linking obesity, Alzheimer's disease, and depression. *The American Journal of Geriatric Psychiatry: Official Journal of the American Association for Geriatric Psychiatry*, 31(10), 853–866. <https://doi.org/10.1016/j.jagp.2023.06.001>
- Maayan, L., Hoogendoorn, C., Sweat, V., & Convit, A. (2011). Disinhibited eating in obese adolescents is associated with orbitofrontal volume reductions and executive dysfunction. *Obesity*, 19(7), 1382–1387. <https://doi.org/10.1038/oby.2011.15>
- McDade, T. W., Reyes-García, V., Tanner, S., Huanca, T., & Leonard, W. R. (2008). Maintenance versus growth: Investigating the costs of immune activation among children in lowland Bolivia. *American Journal of Physical Anthropology*, 136(4), 478–484. <https://doi.org/10.1002/ajpa.20831>
- McDermott, C. L., Seidlitz, J., Nadig, A., Liu, S., Clasen, L. S., Blumenthal, J. D., Reardon, P. K., Lalonde, F., Greenstein, D., Patel, R., Chakravarty, M. M., Lerch, J. P., & Raznahan, A. (2019). Longitudinally mapping childhood socioeconomic status associations with cortical and subcortical morphology. *Journal of Neuroscience*, 39(8), 1365–1373. <https://doi.org/10.1523/JNEUROSCI.1808-18.2018>
- McLaughlin, K. A., Sheridan, M. A., & Lambert, H. K. (2014). Childhood adversity and neural development: Deprivation and threat as distinct dimensions of early experience. *Neuroscience & Biobehavioral Reviews*, 47, 578–591. <https://doi.org/10.1016/j.neubiorev.2014.10.012>
- McLaughlin, K. A., Weissman, D., & Bitrán, D. (2019). Childhood adversity and neural development: A systematic review. *Annual Review of Developmental Psychology*, 1(1), 277–312. <https://doi.org/10.1146/annurev-devpsych-121318-084950>
- Mestre, Z. L., Bischoff-Grethe, A., Eichen, D. M., Wierenga, C. E., Strong, D., & Boutelle, K. N. (2017). Hippocampal atrophy and altered brain responses to pleasant tastes among obese compared with healthy weight children. *International Journal of Obesity*, 41(10), 1496–1502. <https://doi.org/10.1038/ijo.2017.130>
- Miller, J. G., López, V., Buthmann, J. L., Garcia, J. M., & Gotlib, I. H. (2022). A social gradient of cortical thickness in adolescence: Relationships with neighborhood socioeconomic disadvantage, family socioeconomic status, and depressive symptoms. *Biological Psychiatry Global Open Science*, 2(3), 253–262. <https://doi.org/10.1016/j.bpsgos.2022.03.005>
- Mölenberg, F. J. M., Mackenbach, J. D., Poelman, M. P., Santos, S., Burdorf, A., & van Lenthe, F. J. (2021). Socioeconomic inequalities in the food environment and body composition among school-aged children: A fixed-effects analysis. *International Journal of Obesity*, 45(12), 2554–2561. <https://doi.org/10.1038/s41366-021-00934-y>
- Nelson, C. A., & Gabard-Durnam, L. J. (2020). Early adversity and critical periods: Neurodevelopmental consequences of violating the expectable environment. *Trends in Neurosciences*, 43(3), 133–143. <https://doi.org/10.1016/j.tins.2020.01.002>
- Niven, J. E. (2016). Neuronal energy consumption: Biophysics, efficiency and evolution. *Current Opinion in Neurobiology*, 41, 129–135. <https://doi.org/10.1016/j.conb.2016.09.004>
- Noble, K. G., Houston, S. M., Brito, N. H., Bartsch, H., Kan, E., Kuperman, J. M., Akshoomoff, N., Amaral, D. G., Bloss, C. S., Libiger, O., Schork, N. J., Murray, S. S., Casey, B. J., Chang, L., Ernst, T. M., Frazier, J. A., Gruen, J. K., Kennedy, D. N., Van Zijl, P., & Sowell, E. R. (2015). Family income, parental education and brain structure in children and adolescents. *Nature Neuroscience*, 18(5), 773–778. <https://doi.org/10.1038/nn.3983>
- Peters, A., Schweiger, U., Pellerin, L., Hubold, C., Oltmanns, K. M., Conrad, M., Schultes, B., Born, J., & Fehm, H. L. (2004). The selfish brain: Competition for energy resources. *Neuroscience & Biobehavioral Reviews*, 28(2), 143–180. <https://doi.org/10.1016/j.neubiorev.2004.03.002>
- Petersen, A. C., Crockett, L., Richards, M., & Boxer, A. (1988). A self-report measure of pubertal status: Reliability, validity, and initial norms. *Journal of Youth and Adolescence*, 17(2), 117–133. <https://doi.org/10.1007/BF01537962>
- Plachta-Danielzik, S., Bös, Westphal, A., Kehden, B., Gehrke, M. I., Kromeyer-Hauschild, K., Grillenberger, M., Willhöft, C., Heymsfield, S. B., & Müller, M. J. (2013). Adiposity rebound is misclassified by BMI rebound. *European Journal of Clinical Nutrition*, 67(9), 984–989. <https://doi.org/10.1038/ejcn.2013.131>
- Pontzer, H., & McGrosky, A. (2022). Balancing growth, reproduction, maintenance, and activity in evolved energy economies. *Current Biology*, 32(12), R709–R719. <https://doi.org/10.1016/j.cub.2022.05.018>
- R Core Team. (2024). *R: A language and environment for statistical computing* [Computer software]. R Foundation for Statistical Computing. <https://www.R-project.org/>.
- Raichle, M. E., & Gusnard, D. A. (2002). Appraising the brain's energy budget. *Proceedings of the National Academy of Sciences*, 99(16). <https://doi.org/10.1073/pnas.172399499>. Article 16.

- Rakesh, D., & Whittle, S. (2021). Socioeconomic status and the developing brain – A systematic review of neuroimaging findings in youth. *Neuroscience & Biobehavioral Reviews*, 130, 379–407. <https://doi.org/10.1016/j.neubiorev.2021.08.027>
- Rakesh, D., Whittle, S., Sheridan, M. A., & McLaughlin, K. A. (2023). Childhood socioeconomic status and the pace of structural neurodevelopment: Accelerated, delayed, or simply different? *Trends in Cognitive Sciences*, 27(9), 833–851. <https://doi.org/10.1016/j.tics.2023.03.011>
- Reh, R. K., Dias, B. G., Nelson, C. A., Kaufer, D., Werker, J. F., Kolb, B., Levine, J. D., & Hensch, T. K. (2020). Critical period regulation across multiple timescales. *Proceedings of the National Academy of Sciences*, 117(38), 23242–23251. <https://doi.org/10.1073/pnas.1820836117>
- Rosen, M. L., Hagen, M. P., Lurie, L. A., Miles, Z. E., Sheridan, M. A., Meltzoff, A. N., & McLaughlin, K. A. (2020). Cognitive stimulation as a mechanism linking socioeconomic status with executive function: A longitudinal investigation. *Child Development*, 91(4). <https://doi.org/10.1111/cdev.13315>
- Rossee, Y. (2012). lavaan: An R package for structural equation modeling. *Journal of Statistical Software*, 48(2), 1–36. <https://doi.org/10.18637/jss.v048.i02>
- Schabdach, J. M., Schmitt, J. E., Sotardi, S., Vossough, A., Andronikou, S., Roberts, T. P., Huang, H., Padmanabhan, V., Ortiz-Rosa, A., Gardner, M., Covitz, S., Bedford, S. A., Mandal, A. S., Chaiyachati, B. H., White, S. R., Bullmore, E., Bethlehem, R. A. I., Shinohara, R. T., Billot, B., & Alexander-Bloch, A. (2023). Brain growth charts for quantitative analysis of pediatric clinical brain MRI scans with limited imaging pathology. *Radiology*, 309(1), Article e230096. <https://doi.org/10.1148/radiol.230096>
- Sharma, A. K., Metzger, D. L., Daymont, C., Hadjiyannakis, S., & Rodd, C. J. (2015). LMS tables for waist-circumference and waist-height ratio Z-scores in children aged 5–19 y in NHANES III: Association with cardio-metabolic risks. *Pediatric Research*, 78(6), 723–729. <https://doi.org/10.1038/pr.2015.160>
- Shattuck-Heidorn, H., Reiches, M. W., Prentice, A. M., Moore, S. E., & Ellison, P. T. (2017). Energetics and the immune system: Trade-offs associated with non-acute levels of CRP in adolescent Gambian girls. *Evolution, Medicine, and Public Health*, 2017(1), 27–38. <https://doi.org/10.1093/emph/eow034>
- Sheridan, M. A., & McLaughlin, K. A. (2014). Dimensions of early experience and neural development: Deprivation and threat. *Trends in Cognitive Sciences*, 18(11). <https://doi.org/10.1016/j.tics.2014.09.001>. Article 11.
- Taylor, R. L., Cooper, S. R., Jackson, J. J., & Barch, D. M. (2020). Assessment of neighborhood poverty, cognitive function, and prefrontal and hippocampal volumes in children. *JAMA Network Open*, 3(11). <https://doi.org/10.1001/jamanetworkopen.2020.23774>. e2023774.
- Taylor, R. W., Williams, S. M., Carter, P. J., Goulding, A., Gerrard, D. F., & Taylor, B. J. (2011). Changes in fat mass and fat-free mass during the adiposity rebound: FLAME study. *International Journal of Pediatric Obesity*, 6(2–2), e243–e251. <https://doi.org/10.3109/17477166.2010.549488>
- Urlacher, S. S., Ellison, P. T., Sugiyama, L. S., Pontzer, H., Eick, G., Liebert, M. A., Cepon-Robins, T. J., Gildner, T. E., & Snodgrass, J. J. (2018). Tradeoffs between immune function and childhood growth among Amazonian forager-horticulturalists. *Proceedings of the National Academy of Sciences*, 115(17). <https://doi.org/10.1073/pnas.1717522115>. Article 17.
- von Stumm, S., Rimfeld, K., Dale, P. S., & Plomin, R. (2020). Preschool verbal and nonverbal ability mediate the association between socioeconomic status and school performance. *Child Development*, 91(3), 705–714. <https://doi.org/10.1111/cdev.13364>
- Wells, J. C. K. (2023). Natural selection and human adiposity: Crafty genotype, thrifty phenotype. *Philosophical Transactions of the Royal Society B: Biological Sciences*, 378 (1885). <https://doi.org/10.1098/rstb.2022.0224>, 20220224.
- WHO Multicentre Growth Reference Study Group. (2006). *WHO child growth standards: Length/height-for age, weight-for-age, weight-for-height and body mass index-for-age: Methods and development*. Geneva: World Health Organization. https://cdn.who.int/media/docs/default-source/child-growth/growth-reference-5-19-years/computation.pdf?sfvrsn=c2ff6a95_4.
- Yang, J., Liu, H., Wei, D., Liu, W., Meng, J., Wang, K., Hao, L., & Qiu, J. (2016). Regional gray matter volume mediates the relationship between family socioeconomic status and depression-related trait in a young healthy sample. *Cognitive, Affective, & Behavioral Neuroscience*, 16(1), 51–62. <https://doi.org/10.3758/s13415-015-0371-6>
- Zarnowiecki, D. M., Dollman, J., & Parletta, N. (2014). Associations between predictors of children's dietary intake and socioeconomic position: A systematic review of the literature. *Obesity Reviews*, 15(5), 375–391. <https://doi.org/10.1111/obr.12139>